J Mater Sci (2012) 47:429–432
DOI 10.1007/s10853-011-5816-x

Dielectric and elastic properties of 0.70Pb($Mg_{1/3}Nb_{2/3}$)O_3–0.30$PbTiO_3$ single crystal and their electric-field dependence

Zhu Wang · Rui Zhang · Enwei Sun · Wenwu Cao

Received: 24 February 2011 / Accepted: 21 July 2011 / Published online: 4 August 2011

Abstract The dielectric and elastic properties of $[001]_c$-oriented 0.7Pb($Mg_{1/3}Nb_{2/3}$)O_3–0.3$PbTiO_3$ (PMN–0.3PT) crystal were investigated as a function of poling field at 300 and 360 K, respectively. At 300 K, the dielectric constant and elastic compliance of rhombohedral PMN–0.3PT crystal change drastically at a critical field corresponding to an electric-induced ferroelectric phase transition. At 360 K, the PMN–0.3PT crystal is tetragonal, its dielectric constant and elastic compliance change drastically at two critical fields, which indicates an intermediate phase. Furthermore, much small dielectric loss factors and mechanical loss factors are observed in mono-domain state, which indicates that losses mainly come from domain wall contributions.

Introduction

Relaxor-based ferroelectric single crystals, such as $(1-x)$Pb($Mg_{1/3}Nb_{2/3}$)O_3–$x$$PbTiO_3$ (PMN–xPT) and $(1-x)$Pb($Zn_{1/3}Nb_{2/3}$)O_3–$x$$PbTiO_3$ (PZN–xPT), exhibit excellent electromechanical properties in the $[001]_c$ poled Pb($Mg_{1/3}Nb_{2/3}$)O_3–0.33$PbTiO_3$ (PMN–0.33PT) single crystal, with very large longitudinal piezoelectric coefficient d_{33} (2820 pC/N) and super high electromechanical coupling coefficient k_{33} (0.94) [1–3]. In addition to the high electromechanical properties, the crystal exhibits low dielectric loss factor [4, 5]. The combination of high piezoelectric properties and low loss make single crystals excellent components for the actuators, ultrasonic motors, and wideband medical ultrasonic transducers etc.

There were some experimental and theoretical studies on the relationship between electromechanical properties and domain switching phenomena [6–9]. It is found that the high piezoelectric coefficient observed in these multi-domain single crystals is related to the polarization rotation when an electric field is applied along the nonpolar $[001]_c$ direction of the rhombohedral phase single crystal [10–16]. Moreover, the macroscopic properties of relaxor-based ferroelectric single crystal are strongly related to their domain structures, which are greatly influenced by temperature and electric field conditions [17, 18].

In this study, the dependence of dielectric and elastic properties of Pb($Mg_{1/3}Nb_{2/3}$)O_3–0.3$PbTiO_3$ (PMN–0.3PT) single crystal on poling field were measured at 300 and 360 K, and the correlation between the electromechanical properties and domain structure has been investigated.

Experimental

The PMN–0.3PT single crystal used in this study was grown by the modified Bridgman technique [19], which was purchased from Shanghai Institute of Ceramics, Chinese Academy of Sciences. The sample was oriented, cut, and polished into k_{31} resonator with dimensions of $9.65\,\text{mm}//[100]_c^L \times 1.20\,\text{mm}//[010]_c^W \times 0.35\,\text{mm}//[001]_c^T$. Then, the sample was sputtered with gold electrodes on the pair of $[001]_c$ surfaces.

Z. Wang · R. Zhang (✉) · E. Sun · W. Cao
Center for the Condensed Matter Science and Technology, Department of Physics, Harbin Institute of Technology, Harbin, Heilongjiang 150080, China
e-mail: ruizhang_ccmst@yahoo.com.cn; ruizhang_ccmst@hit.edu.cn

W. Cao
Materials Research Institute, The Pennsylvania State University, University Park, PA 16802, USA

In the experiments, the sample was first heated and maintained at 530 K for 2 h to depole the crystal, then cooled down to room temperature slowly without field to release the internal stresses. Afterward, the sample was poled stepwise with increasing electric field. In order to achieve a quasi-static condition, the whole measurement process took about 5 h to complete. The dielectric constant ε_{33}^{T} and dielectric loss factor tgδ were measured at 1 kHz by an impedance analyzer (Agilent 4294A, Precision Impedance Analyzer) and a DC bias test fixture (Agilent 16065A). The elastic compliance s_{11}^{E} and mechanical loss factor tgϕ of PMN–0.3PT crystal were calculated from the admittance spectra following the procedure described in Ref. [20]. The remnant polarization P_r was measured by Precision Premier II (Radiant Technologies).

Results and discussion

Figure 1 shows the dependence of dielectric constant of rhombohedral PMN–0.3PT single crystal on the poling field measured at 300 K. The dielectric constant ε_{33}^{T} decreases slightly at 60 V/mm. Upon further increase of the poling field, ε_{33}^{T} increases drastically at 100 V/mm and reaches a maximum value at $\sim$180 V/mm due to domain switching.

The elastic compliance generally changes drastically at the electric-induced ferroelectric phase transition [5], so that the drastic change of elastic compliance can be used to define the critical field of electric-induced ferroelectric phase transition. Figure 2 shows the dependence of elastic compliance on poling field measured at 300 K. Resonance peaks appear in the admittance spectra at 45 V/mm, indicating that some domains begin to switch, producing non-zero polarization. The elastic compliance s_{11}^{E} reaches 38×10^{-12} m^2/N at 100 V/mm, and then increases abruptly to 45×10^{-12} m^2/N at 110 V/mm. Meanwhile,

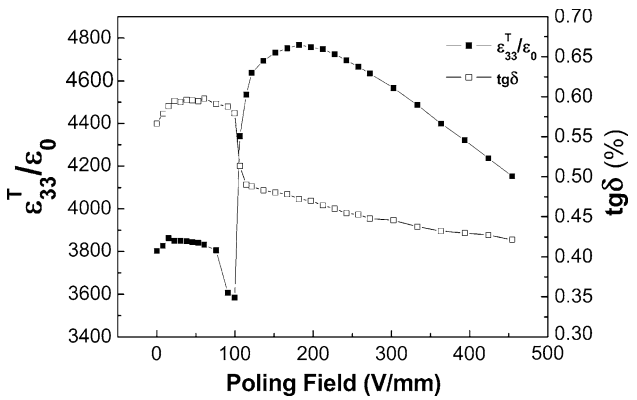

Fig. 1 The dielectric constant ε_{33}^{T} and dielectric loss factor tgδ of PMN–0.3PT as a function of poling field measured at 300 K

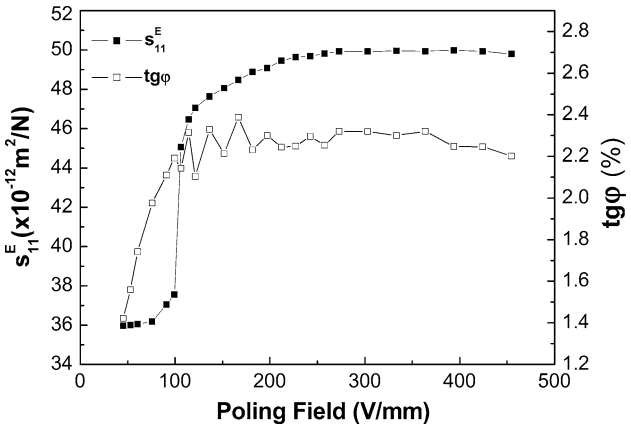

Fig. 2 The elastic compliance s_{33}^{E} and mechanical loss factor tgϕ of PMN–0.3PT as a function of poling field measured at 300 K

the mechanical loss factor tgϕ jumps from 1.4 to 2.1%. Based on the drastic change of elastic compliance, the critical field of the sample is found to be 100 V/mm at 300 K.

As shown in Fig. 3, the remnant polarization P_r exhibits a peak at 360 K corresponding to the ferroelectric phase transition from rhombohedral to tetragonal phase, which has been previously confirmed experimentally [11, 21], while the abrupt change at 410 K indicates the phase transition from tetragonal ferroelectric phase to cubic paraelectric phase.

Figures 4 and 5 show the dependence of dielectric constant and elastic compliance on the poling field measured at 360 K. As shown in Fig. 4, a peak of the dielectric constant ε_{33}^{T} is obtained at 70 V/mm. Upon further increase of the electric field, ε_{33}^{T} and tgδ decrease to 5770 and 0.44%, respectively, at 120 V/mm. And then ε_{33}^{T} and tgδ decrease drastically at 210 V/mm, and reach 2640 and 0.25%, respectively, at 270 V/mm.

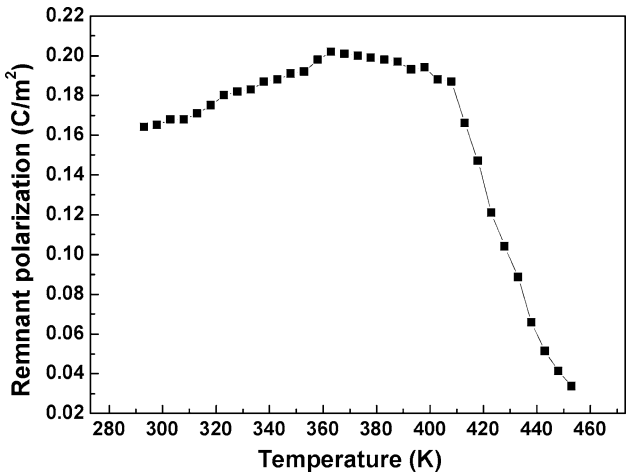

Fig. 3 Temperature dependence of remnant polarization P_r of unpoled PMN–0.3PT single crystal

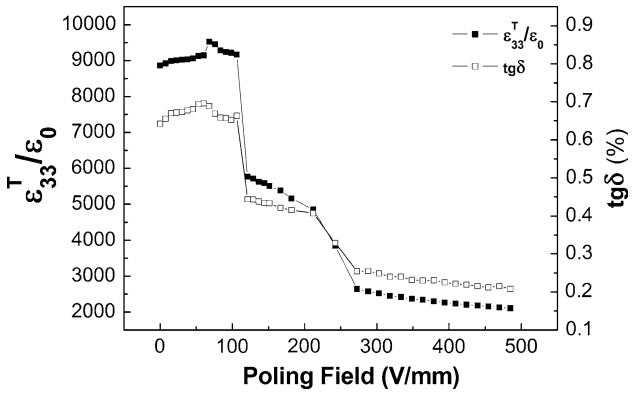

Fig. 4 The dielectric constant ε_{33}^{T} and dielectric loss factor tgδ of PMN–0.3PT as a function of poling field measured at 360 K

At 360 K, $[001]_c$ direction is one of polar axes of the tetragonal phase PMN–0.3PT single crystal. Mono-domain state can be obtained in the PMN–*x*PT crystals if the poling field is sufficiently large along the polar axes [22, 23]. In the $[001]_c$-cut PMN–0.4PT crystal studied previously, the domain switching process was identified as (T_{100} or T_{010}) → M → T_{001}, i.e., a monoclinic phase serves as an intermediate phase. Similar polarization rotation occurs in $[001]_c$-oriented PMN–0.3PT at a field level as small as 270 V/mm when the crystal is tetragonal at 360 K [11]. Similar phenomenon was also observed in PZN–0.09PT single crystal [24].

As shown in Fig. 5, the s_{11}^{E} decreases drastically at two critical fields: 70 and 210 V/mm. The tgϕ increases drastically within 70 V/mm. As the electric field increases, the tgϕ reaches a plateau, then decreases drastically at 210 V/mm as the crystal approaches the mono-domain state. In order to explain this phenomenon, the role of domains and domain walls in the single crystal must be considered. There are two types of domains: the 180° and non-180° ferroelectric domains [25, 26]. The strain tensors are the same for the two domains connected by an 180° domain wall, so that this kind of domain walls only contribute to the polarization and dielectric properties [27]. The non-180° domain walls refer to walls between domains of different strain tensor. In general, both 180° and non-180° domains form to reduce the effects of depolarization field, whereas only non-180° domains contribute to the minimization of the elastic energy [4]. Thus, the dielectric loss is originated from both the 180° and non-180° domain wall motions, while the mechanical loss originates only from non-180° domain wall motions.

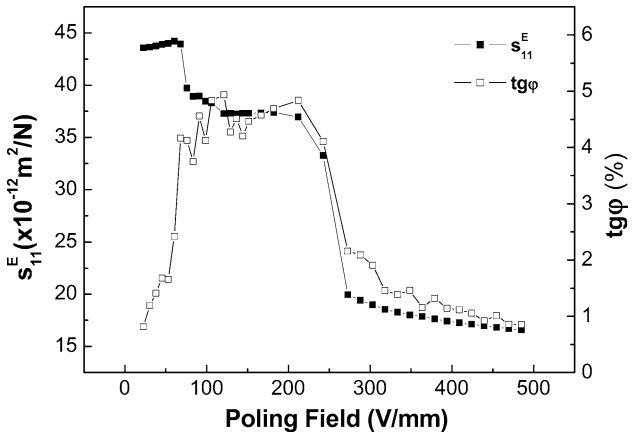

Fig. 5 The elastic compliance s_{33}^{E} and mechanical loss factor tgϕ of PMN–0.3PT as a function of poling field measured at 360 K

For $[001]_c$-cut PMN–0.3PT single crystal, tgδ decreases during the poling at 300 K, but tgϕ increases due to the addition of non-180° domain walls [28, 29]. Moreover, the 180° domain switching could be accomplished through two consecutive non-180° domain switching as observed experimentally through ultrasonic velocity measurements [5]. At 360 K, there are no more contributions from domain walls when the crystal is poled into mono-domain state beyond 270 V/mm, so that both dielectric and mechanical loss factors become very small.

Summary and conclusion

In this study, domain switching phenomena during the poling have been systematically investigated through the measurement of dielectric constant and elastic compliance. At 360 K, the dielectric constant and elastic compliance of the $[001]_c$ poled PMN–0.3PT crystal change drastically at two critical fields, which indicates the presence of an intermediate phase between up and down domain states. Based on the fact that the dielectric loss factor decreases while the mechanical loss factor initially increases when the switching begin, we conclude that there is no direct 180° domain switching during the poling. Instead, two consecutive non-180° domain switching is the primary route to accomplish the poling.

Acknowledgements This research was supported in part by the NSFC under Grant No. 50972034, Program of the Ministry of Education of China for New Century Excellent Talents in University under Grant No. NCET-06-0345, Postdoctoral Science Research Developmental Foundation of Heilongjiang Province under Grant No. LBH-Q06068, program of BRET2.2010004 and excellent Team in Harbin Institute of Technology, SRF for ROCS, SEM, and NIH Grant No. P41-EB21820.

References

1. Park SE, Shrout TR (1997) J Appl Phys 82:1804
2. Zhang R, Jiang B, Cao WW (2001) J Appl Phys 90:3471
3. Liu XZ, Zhang SJ, Luo J, Shrout TR, Cao WW (2009) J Appl Phys 106:074112

4. Zhang SJ, Sherlock NP, Meyer RJ Jr, Shrout TR (2009) Appl Phys Lett 94:162906
5. Yin JH, Cao WW (2002) Appl Phys Lett 80:1043
6. Viehland D, Chen YH (2000) J Appl Phys 88:6696
7. Lente MH, Eiras JA (2001) J Appl Phys 89:5093
8. Viehland D, Li F (2002) J Appl Phys 92:7690
9. Tu CS, Shih IC (2003) Appl Phys Lett 83:1833
10. Fu H, Cohen RE (2001) Nature 403:281
11. Davis M, Damjanovic D, Setter N (2006) Phys Rev B 73:014115
12. Noheda B, Cox DE, Shirane G, Park SE, Cross LE, Zhong Z (2001) Phys Rev Lett 86:3891
13. Li SP, Cao WW, Newnham RE, Cross LE (1993) Ferroelectrics 139:25
14. Robels U, Herbiet R, Arlt G (1989) Ferroelectrics 93:95
15. Uchino K, Hirose S (2001) IEEE Trans Ultrason Ferroelectr Freq Control 48:207
16. Bai F, Wang N, Li J, Viehland D, Gehring PM, Xu G, Shirane G (2004) J Appl Phys 96:1620
17. Zhang SJ, Luo J, Hackenberger W, Sherlock NP, Meyer RJ Jr, Shrout TR (2009) J Appl Phys 105:104506
18. Tu CS, Tsai CL, Chen JS, Schmidt VH (2002) Phys Rev B 65:104113
19. Yin ZW, Luo HS, Wang PC, Xu GS (1999) Ferroelectrics 229:207
20. Wang Z, Zhang R, Sun ES, Cao WW (2010) J Appl Phys 107:014110
21. Tu CS, Chuang HT, Lee SC, Chien RR, Schmidt VH, Luo H (2008) J Appl Phys 104:024110
22. Chien RR, Tu CS, Schmidt VH, Wang FT (2006) J Phys Condens Matter 18:8337
23. Chien RR, Schmidt VH, Hung LW, Tu CS (2005) J Appl Phys 97:114112
24. Xiang Y, Zhang R, Cao WW (2011) J Mater Sci 46:1839. doi: 10.1007/s10853-010-5009-z
25. Han J, Cao WW (2003) Appl Phys Lett 83:2040
26. Bokov AA, Ye ZG (2004) J Appl Phys 95:6347
27. Damjanovic D (2005) In: Mayergoyz I, Bertolli G (eds) The science of hysteresis, vol 3. Elsevier, New York
28. Kamel TM, de With G (2007) J Appl Phys 102:044118
29. Li S, Bhalla S, Newnham RE, Cross LE, Huang C (1994) J Mater Sci 29:1290. doi:10.1007/BF00975077